JACS
JOURNAL OF THE AMERICAN CHEMICAL SOCIETY
Article
Cite This: J. Am. Chem. Soc. XXXX, XXX, XXX−XXX
pubs.acs.org/JACS

Lithium Amino Alkoxide−Evans Enolate Mixed Aggregates: Aldol Addition with Matched and Mismatched Stereocontrol

Janis Jermaks, Evan H. Tallmadge, Ivan Keresztes, and David B. Collum*

Department of Chemistry and Chemical Biology Baker Laboratory, Cornell University Ithaca, New York 14853-1301, United States

Supporting Information

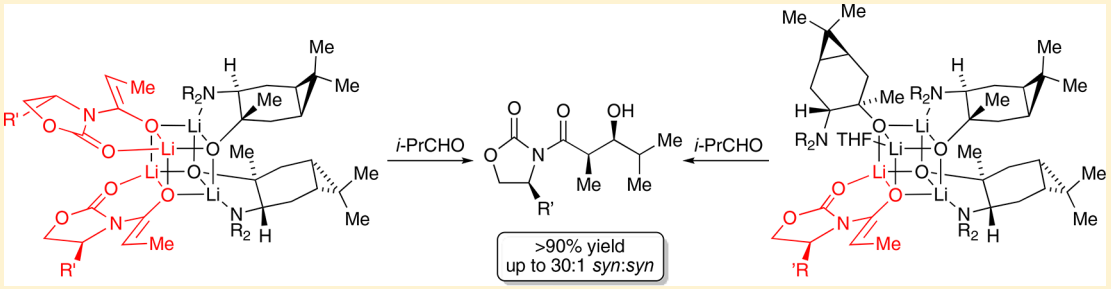

ABSTRACT: Building on structural and mechanistic studies of lithiated enolates derived from acylated oxazolidinones (Evans enolates) and chiral lithiated amino alkoxides, we found that amino alkoxides amplify the enantioselectivity of aldol additions. The pairing of enantiomeric series affords matched and mismatched stereoselectivities. The structures of mixed tetramers showing 2:2 and 3:1 (alkoxide-rich) stoichiometries are determined spectroscopically. Rate and computational studies provide a viable mechanistic and stereochemical model based on the direct reaction of the 3:1 mixed tetramers, but they raise unanswered questions for the 2:2 mixed aggregates.

INTRODUCTION

This paper describes the influence of chiral lithiated amino alkoxides on the aldol addition of oxazolidinone-derived lithium enolates (eq 1). The story begins with the seminal 1981 paper by Evans and co-workers describing remarkably selective aldol additions by the boron enolate of a chiral oxazolidinone.[1] The impact of Evans' paper would be difficult to overstate. Applications and subsequent refinements of the so-called Evans aldol and related stereoselective functionalizations of "Evans enolates" are legion.[2] One might surmise that lithiated Evans enolates would be central to the plotline,[3] but they reside between the more reactive sodium enolates used in alkylations[4] and the more selective transition-metal and boron enolates used for aldol additions.[5] Nonetheless, there are a handful of lithium-based Evans aldol additions, and surprisingly, many are additions to ketones[6] rather than aldehydes.[7]

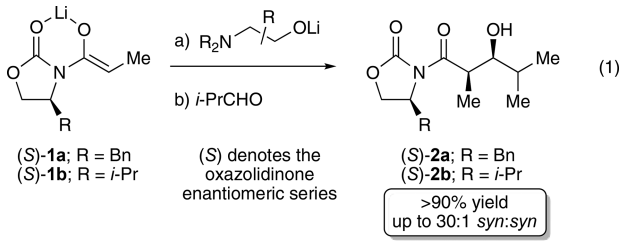

(1)

In recent studies, we found that aldol additions to isobutyraldehyde (*i*-PrCHO) and cyclohexanone afford credible selectivities and yields (Scheme 1).[8] Pronounced aging effects[9]—the influence of time and warming on enolate reactivity before the addition of the electrophile—may have bedeviled synthetic chemists, including a Pfizer process group working on plant scales.[6] Independent of the enolate aging effects and in stark contrast to conventional wisdom based on simpler aldol additions,[10] the aldolate derived from *i*-PrCHO is susceptible to a retroaldol reaction that causes a loss of yield and selectivity. However, the cyclohexanone-derived aldolate is robust.[8]

Scheme 1. Aldol Additions of Lithiated Evans Enolates

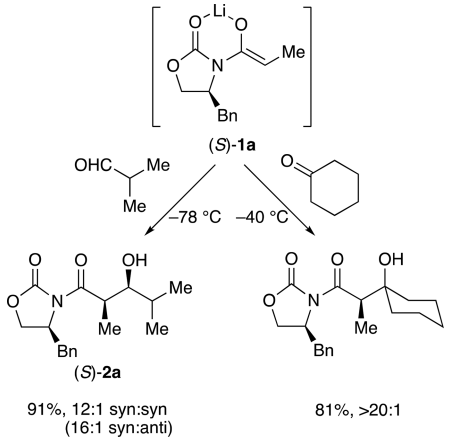

The aging effects of enolate (*S*)-**1a** were traced to kinetically formed and highly reactive trisolvated dimers **3** and **4**, which

Received: December 29, 2017

DOI: 10.1021/jacs.7b13776
J. Am. Chem. Soc. XXXX, XXX, XXX−XXX

Scheme 2. Structures of Evans Enolates and Mechanism of Aldol Additions

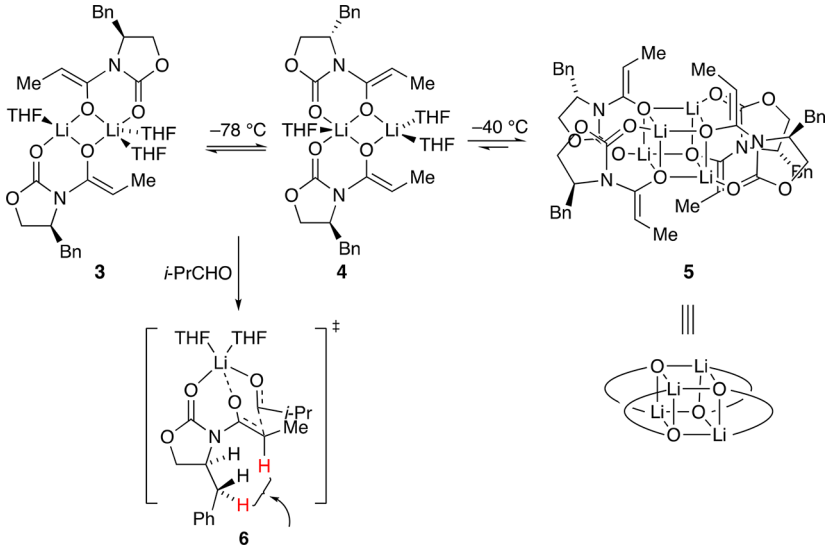

formed unreactive unsolvated tetramer **5** on standing at −78 °C or with gentle warming (Scheme 2).[8] Rate and computational studies implicated monomer-based transition structure **6**. We would be remiss if we did not also mention that computational studies suggested that the H−H interaction highlighted in **6** causes facial selectivity rather than an explicit interaction of the aldehyde with the benzyl moiety. This outcome, too, appears to be incongruent with conventional thinking.

An increasingly popular and altogether different means of controlling enantioselectivities involves noncovalent auxiliaries—chiral salts that form mixed aggregates in situ.[11,12] Such a strategy relies on controlling the complex coordination chemistry of mixed aggregates, which usually requires a combination of determination and luck. An iconic example was reported by the process group at Merck in 1995: an equimolar (2:2) mixture of lithium acetylide **7** and chiral amino alkoxide **8** were added to a ketone with an astonishing 50:1 enantioselectivity en route to 50000 kg of the reverse transcriptase inhibitor efavirenz (eq 2).[13] The Merck group also noted aging effects in which warming before the addition of the ketone was required to optimize the selectivity. In a collaborative effort, we traced the selectivities and aging effects to the slow formation of C_2-symmetric 2:2 mixed aggregate **9** and direct 1,2-addition via transition structure **10**.[14]

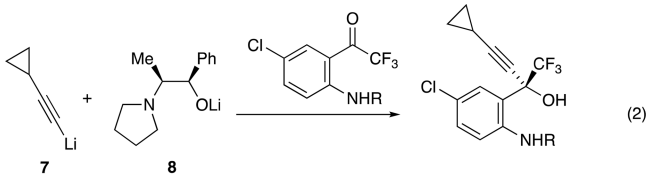

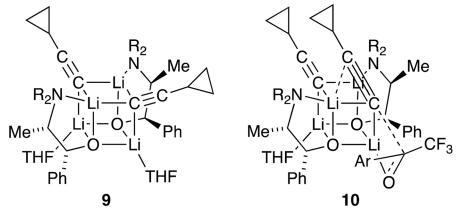

Second-generation reverse transcriptase inhibitors developed at DuPont Pharmaceuticals (now Bristol-Myers Squibb) were prepared by adding lithium acetylides to quinazolinones (eq 3).[15]

Despite its apparent similarity to the Merck chemistry, the DuPont process relied on caranolate-derived amino alkoxide **11** using 3:1 rather than 2:2 stoichiometry. Structural studies showed the intermediacy of 3:1 (alkoxide-rich) mixed aggregate **12** with a proposed extra-aggregate addition of lithium acetylide.[16] Optimizations afforded 2000 kg of the adduct in >200:1 enantioselectivity before the program was terminated.[17]

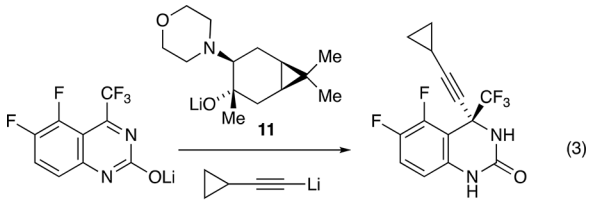

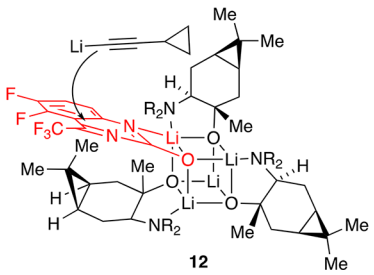

We neither had the skills contemporaneous to the DuPont and Merck studies to characterize amino alkoxides **8** and **11** nor were they needed.[13−17] A dozen years later, however, we characterized them as fully chelated tetramers **13** and **14** with S_4-symmetric cores (Scheme 3).[18] The structures prompted us to ask whether the inherent selectivity of Evans enolates can be amplified by their incorporation into cubic mixed aggregates with chiral alkoxides. It was unclear at the outset whether mixed aggregation would afford discrete structures given the difference in the core symmetries of the enolates and alkoxides, D_{2d} versus S_4. Moreover, the favorable stereochemical influence was in doubt given that homotetrameric enolate **5** reacts sluggishly via a fleeting monomer rather than via a tetramer.[19] In short, we got lucky: tetrameric mixed aggregates form with excellent structural control and react rapidly without dissociation (Scheme 4). This success is by no means simple when viewed in detail. The nonspecialist will find summaries of the results in the Discussion.

DOI: 10.1021/jacs.7b13776
J. Am. Chem. Soc. XXXX, XXX, XXX−XXX

Scheme 3. Structures of Amino Alkoxide Homotetramers

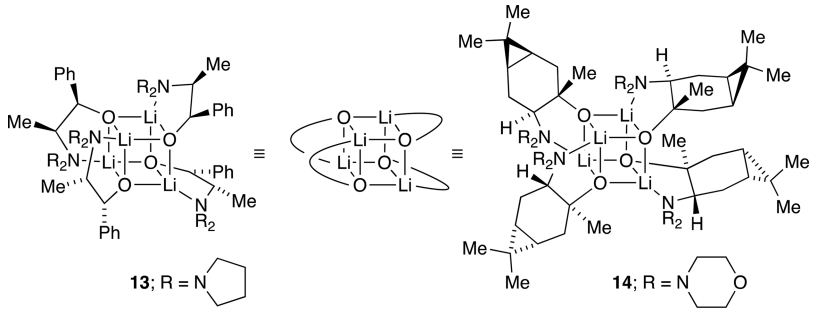

Scheme 4. Evans Aldol Addition of Lithium Enolate Mixed Aggregates

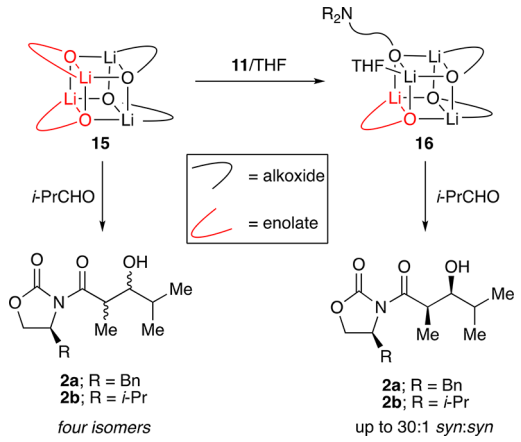

RESULTS

Structure Determination: General. The characterization of the enolate–alkoxide mixed tetramers required a multipronged approach. Mixed aggregates often display characteristic symmetries (or lack thereof). Symmetry can be broken further using the method of continuous variations,[20] also known as the method of Job,[21] which has been central to our studies of homoaggregates.[22] Although heteroaggregates and mixed aggregates[23] often distribute statistically,[22] several unusual nonstatistical examples are described below. Pairings of (*S*)-**1a,b** and alkoxides **8** or **11** and the subsequent formation of aldol adducts (*S*)-**2a,b** are complemented by pairings with antipodal enolates (*R*)-**1a,b**.

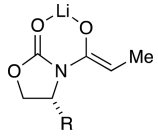

(*R*)-**1a**; R = Bn
(*R*)-**1b**; R = *i*-Pr

Stereoisomers of aggregates can be distinguished using two-dimensional NMR spectroscopies (COSY, TOCSY, HSQC, HMBC, and ROESY).[24] Detailed discussions of the cross-correlations without an interactive computer interface are beyond the scope of this (or essentially any) paper; the analyses are archived in the Supporting Information. We have, however, provided a series of videos rendering the process more tractable. Li–N contacts are shown with ^{6}Li–^{15}N coupling using [^{6}Li,^{15}N]**11**. Density functional theory (DFT) calculations to probe both reactant and transition structures were carried out at the B3LYP/6-31G(d) level with energies from single-point calculations at the MP2 level of theory.[25]

Most of our efforts focused on carane-derived alkoxide **11** and antipodes of enolates **1a,b**, but we also undertook more limited studies of ephedrate-derived alkoxide **8**. We begin with a brief description of the results for a simple enolate to establish baseline behaviors. All of the samples described herein required aging at 25 °C for 10 min to ensure the full equilibration of the aggregates.[26]

Lithium Cyclohexenolate (*Cy*OLi)–Caranolate Derived Mixed Tetramers. Mixtures of *Cy*OLi and lithium alkoxide (ROLi) **11** in tetrahydrofuran (THF) at varying alkoxide/enolate proportions produced ^{6}Li NMR spectra (Figure 1) consistent with

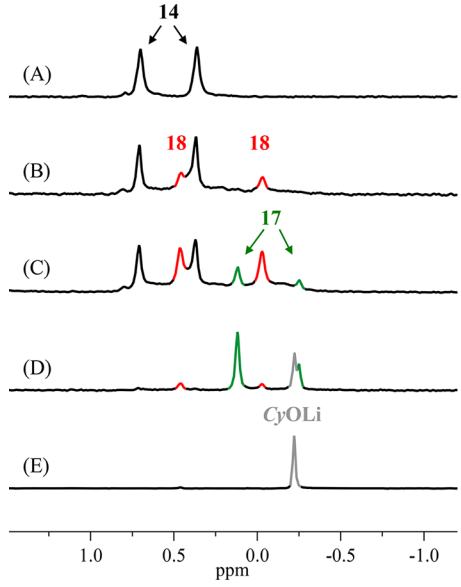

Figure 1. ^{6}Li NMR spectra of 0.10 M solutions of lithium cyclohexenolate (*Cy*OLi) and **11** in toluene and 0.11 M tetrahydrofuran (THF) at −80 °C with 0.11 M [^{6}Li] lithium diisopropylamide ([^{6}Li]LDA). The measured mole fractions[27] of *Cy*OLi (χ_{CyOLi}) are 0.00, 0.13, 0.32, 0.78, and 1.00 for A–E, respectively.

1:3 (enolate-rich) and 2:2 mixed tetramers (**17** and **18**) in analogy with the ROLi-acetylide described above.[13–17] Tetramer **17** was uniquely consistent with the 1:3 stoichiometry and symmetry. There were, however, two computationally less viable

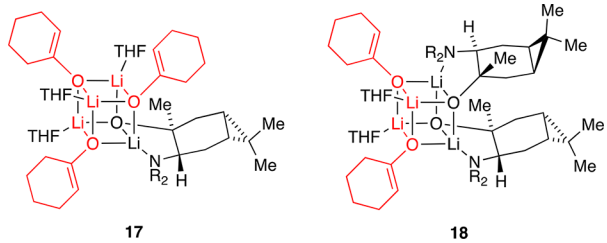

17 **18**

DOI: 10.1021/jacs.7b13776
J. Am. Chem. Soc. XXXX, XXX, XXX–XXX

isomers of **18** (not shown). No 3:1 (alkoxide-rich) aggregates were detectable. A Job plot shows some preference for **17** (Figure 2).

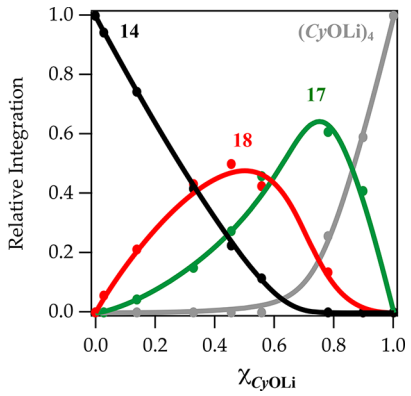

Figure 2. Job plot showing relative integration of the ^{6}Li resonances $(Cy\text{OLi})_4$[22] (gray), **14** (black), **17** (green), and **18** (red) versus the measured mole fraction of *Cy*OLi ($\chi_{Cy\text{OLi}}$) monitored with ^{6}Li NMR spectroscopy in 0.11 M THF/toluene at −80 °C. The total lithium alkoxide titer (enolate and alkoxide) is constant (0.10 M).

A distribution of homotetramers and two of three possible mixed tetramers that is otherwise statistical is shown in Figure 3 for comparison.

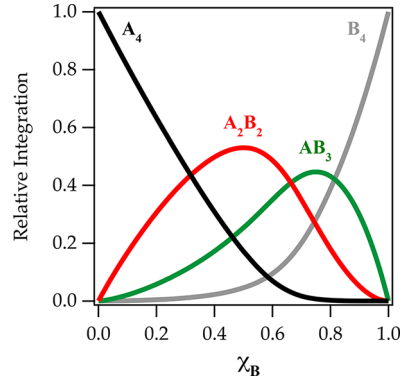

Figure 3. Simulated Job plot showing a statistical distribution of aggregates $\mathbf{A}_4$ (black), $\mathbf{A}_2\mathbf{B}_2$ (red), $\mathbf{AB}_3$ (green), and $\mathbf{B}_4$ (gray) versus the measured mole fraction of **B** (χ_B) for an $\mathbf{A}_4 \rightleftharpoons \mathbf{A}_2\mathbf{B}_2 \rightleftharpoons \mathbf{AB}_3 \rightleftharpoons \mathbf{B}_4$ ensemble.

Structures of Caranolate-Derived Mixed Tetramers. Combining an Evans enolate—(*S*)-**1a**, (*R*)-**1a**, (*S*)-**1b**, or (*R*)-**1b**—with amino alkoxide **11** produced mixed tetramers (*S*)-**15a,b**, (*R*)-**15a,b**, (*S*)-**16a,b**, and (*R*)-**16a,b** (Chart 1) in proportions that depended intimately on the choice of toluene versus THF. The phenylalanine-derived "**a**" series and valine-derived "**b**" series displayed similar spectroscopic behaviors. Mixed aggregates in the **a** series are described emblematically as follows.

An equimolar (1:1) mixture of (*S*)-**1a** and alkoxide **11** in toluene (Figure 4A,E) afforded a complex distribution of species that, on warming to 25 °C for 10 min and cooling to −80 °C, converged to 2:2 mixed tetramer (*S*)-**15a** with high fidelity (Figure 4C). Surprisingly, neither 3:1 nor 1:3 mixed tetramers were observed at any stoichiometry (Figure 4B,D). When [^{15}N]**11** was used, the downfield resonance of (*S*)-**15a** appeared as a doublet (1.39 ppm, $J_{\text{Li–N}}$ = 2.8 Hz) with an accompanying 1:1:1 triplet in the ^{15}N spectrum. This result is consistent with fully chelating amino alkoxide subunits in (*S*)-**15a**.

The 1:1 pair of ^{6}Li resonances did *not* distinguish symmetric mixed tetramer (*S*)-**15a** from a simpler mixed dimer. To this end,

Chart 1. Mixed Tetramers with 2:2 and 3:1 (Alkoxide-Rich) Stoichiometry

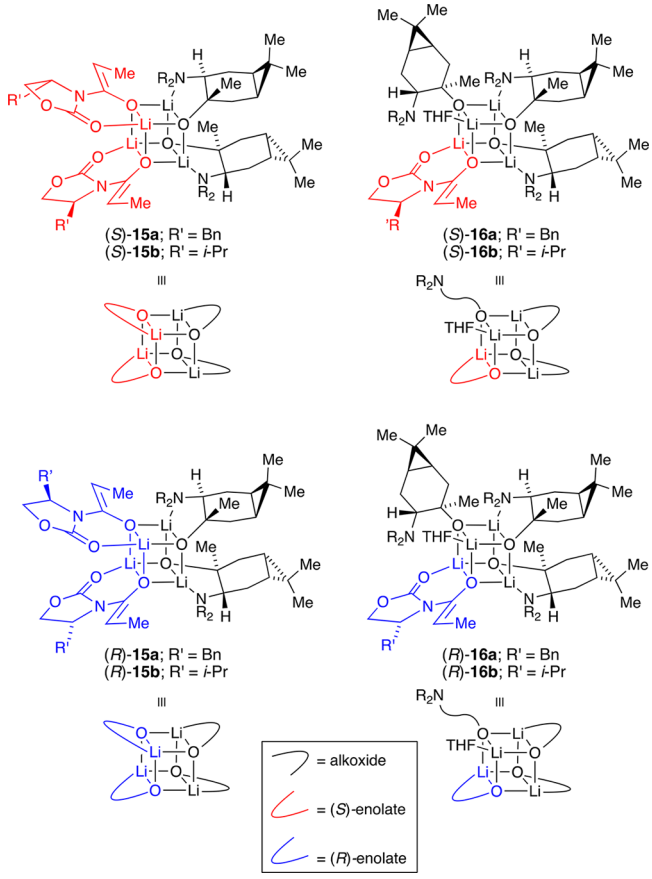

the ^{6}Li spectra of a 1:1 mixture of alkoxide **11** and lithium enolate in which the enolate was equal parts (*S*)-**1a** and (*R*)-**1a** showed four new resonances (1:1:1:1; Figure 5) consistent with desymmetrized mixed tetramer **19** (eq 4). We completed a Job plot by holding the alkoxide/enolate ratio constant (1:1) and monitoring the ^{6}Li spectra versus mole fractions of enolates (*S*)-**1a** and (*R*)-**1a** (Figure 6).

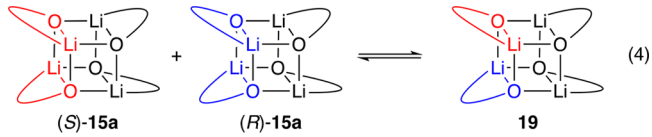

(4)

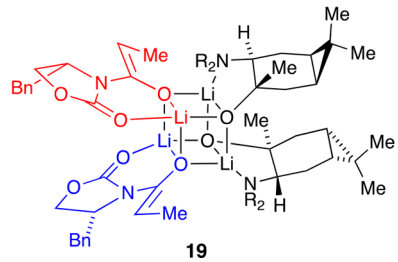

Of course, 2:2 mixed tetramer (*S*)-**15a** is necessarily unsolvated in toluene,[28] and studies with THF suggested that (*S*)-**15a** does not accept coordinating solvents either. Using a control experiment of increasing importance in our laboratory, we added pyridine to toluene solutions to probe lithium ion solvation.[22] The coordination of pyridine to a ^{6}Li nucleus causes a marked (>1.0 ppm) downfield chemical shift of any resonance bearing a coordinated solvent.[29−31] When 1.0 M pyridine was added to (*S*)-**15a**, a new species appeared corresponding to a 3:1 mixed

DOI: 10.1021/jacs.7b13776
J. Am. Chem. Soc. XXXX, XXX, XXX−XXX

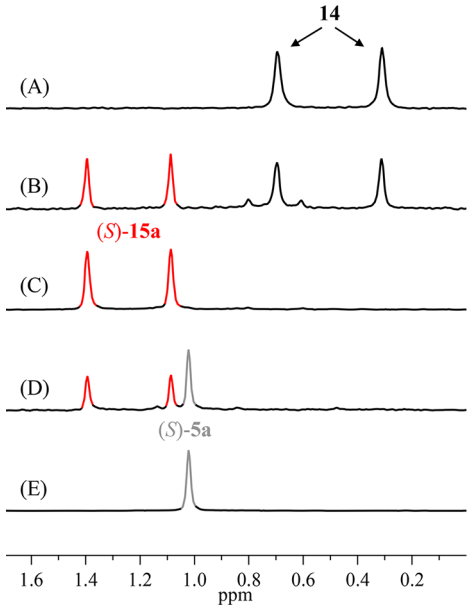

Figure 4. ^{6}Li NMR spectra of 0.10 M solutions of (*S*)-**1a** and **11** in toluene and 0.11 M THF/toluene at −80 °C with 0.11 M [^{6}Li]LDA. The measured mole fractions of (*S*)-**1a** ($\chi_{(S)\text{-}1a}$) are 0.00, 0.24, 0.50, 0.74, and 1.00 for A−E, respectively.

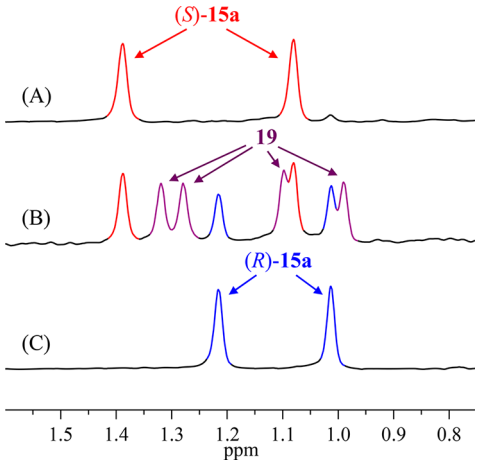

Figure 5. ^{6}Li NMR spectra of 0.10 M solutions containing equimolar alkoxide **11** and enolates (*S*)-**1a** and (*R*)-**1a** (0.050 M constant enolate titer) in 0.11 M THF/toluene at −80 °C: (A) (*S*)-**15a**; (B) 1:1 (*S*)-**15a** and (*R*)-**15a** (1:1); (C) (*R*)-**15a**.

aggregate (vide infra), but it had no measurable effect on the resonances of (*S*)-**15a**.

The assignment of (*S*)-**15a** was completed with the gamut of two-dimensional NMR spectroscopies (Supporting Information). We also examined the efficacy of DFT calculations for distinguishing the five possible stereoisomers of 2:2 mixed aggregates consistent with the ^{6}Li spectroscopic data (one isomer was inconsistent) and obtained the results in Chart 2. The value of 2.2 kcal/mol for the observed form indicated a discrepancy between theory and experiment.

Spectroscopic data of (*R*)-**15a** derived from alkoxide **11** and antipodal enolate (*R*)-**1a** were in every respect analogous to those of (*S*)-**15a** (Supporting Information). Calculations also failed to show the preference for (*R*)-**15a** relative to the isomer analogous to **22** but only by 0.1 kcal/mol.

The solvent-dependent formation of 3:1 mixed aggregates (*S*)-**16a** was observed with a THF titration of a 3:1 mixture of

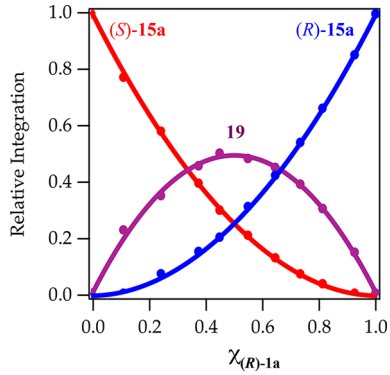

Figure 6. Job plot showing the relative integration of the ^{6}Li resonances of (*S*)-**15a** (red), (*R*)-**15a** (blue), and **19** (purple) versus the measured mole fraction[27] of (*R*)-**1a** [$\chi_{(R)\text{-}1a}$] monitored with ^{6}Li NMR spectroscopy in 0.11 M THF/toluene at −80 °C. The total enolate and alkoxide titer are constant (0.10 M).

Chart 2. Computed Energies of Isomeric 2:2 Mixed Tetramers (Relative kcal/mol)

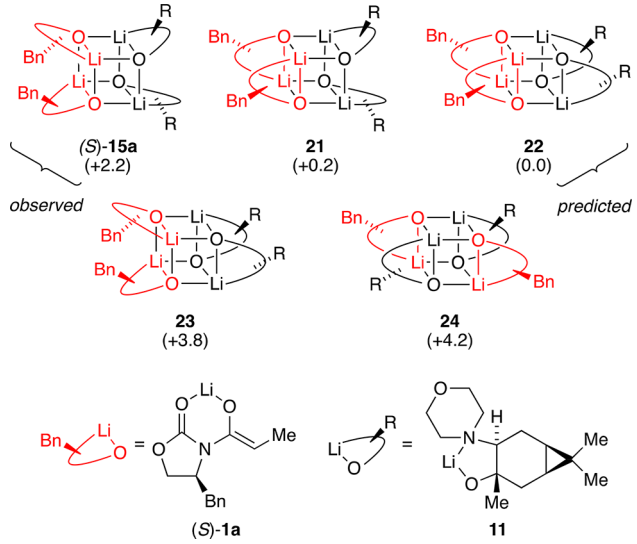

alkoxide **11** and enolate (*S*)-**1a** (eq 5 and Figure 7). In neat toluene, only mixed (*S*)-**15a** and homoaggregated alkoxide tetramer **14** were observed (Figure 7A). During incremental increases in THF concentration, 3:1 mixed tetramer (*S*)-**16a** emerged (Figure 7C) and became the sole observable mixed aggregate in neat THF (Figure 7F). The existence of a single enolate subunit within (*S*)-**16a**, although not in doubt, was confirmed by using a 3:1 mixture of alkoxide and enolate with equal proportions of (*S*)-**1a** and (*R*)-**1a**, which yielded (*S*)-**16a** and (*R*)-**16a** to the exclusion of other species. The existence of two rather than three chelated alkoxides was shown using [^{15}N]**11**, which afforded two ^{6}Li doublets and a ^{6}Li singlet accompanied by two triplets (1:1:1) and a singlet in the ^{15}N NMR spectrum.

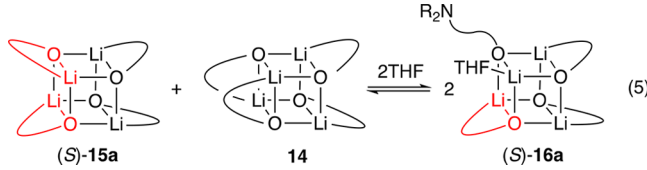

(5)

A coordinated THF was confirmed using several strategies. The addition of 4.0 M pyridine to a THF solution of (*S*)-**16a** at −80 °C resulted in downfield shifts of the four resonances to

DOI: 10.1021/jacs.7b13776
J. Am. Chem. Soc. XXXX, XXX, XXX−XXX

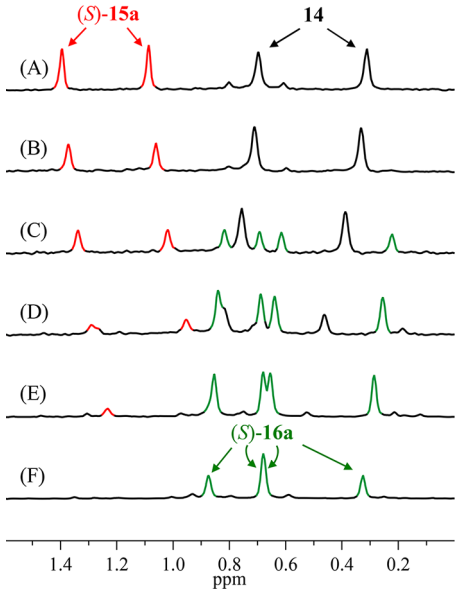

Figure 7. ^{6}Li spectra of a 3:1 mixture of alkoxide **11** (0.075 M) and (*S*)-**1a** (0.025 M) with various concentrations of THF in toluene at −80 °C showing the appearance of THF-solvated aggregate (*S*)-**16a**. Concentrations of THF in toluene are (A) 0.0 M, (B) 1.0 M, (C) 3.0 M, (D) 6.0 M, (E) 9.0 M, and (F) neat THF.

various extents. The shifts were small because the degree of pyridine coordination was low. However, at −105 °C, four resonances corresponding to the pyridine solvate were observed in the slow-exchange limit.[22] In a second experiment, the addition of 2.0 equiv hexamethylphosphoramide (HMPA) per lithium to a THF solution afforded (*S*)-**25a** for which the most upfield resonance appeared as a doublet (0.26 ppm, J_{Li-P} = 4.3 Hz) owing to ^{6}Li − ^{31}P coupling, but no change in the four ^{6}Li chemical shifts was observed.[32]

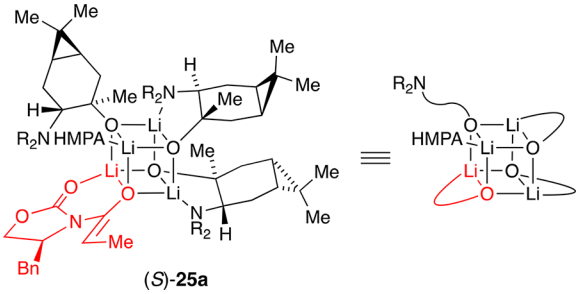

Characterizing (*S*)-**16a** proved a profoundly challenging resolution problem. Fortunately, the full complement of two-dimensional NMR spectroscopies (vide supra) applied to isostructural HMPA solvate (*S*)-**25a** provided a three-dimensional picture that included the preferred orientation of the unchelated alkoxide (Supporting Information). Once again, we exploited DFT to examine the 11 possible isomers of (*S*)-**16a** (Chart 3). In this instance, the computations predicted the observed form to be the most stable. Applying the spectroscopic analysis described above to (*R*)-**1a** provided the structure of (*R*)-**16a**. The computations for the 11 isomers of (*R*)-**16a** solvated by THF matched the spectroscopic results (Supporting Information).

Mixtures of caranolate alkoxide **11** and valine-derived enolates (*R*)-**1b** or (*S*)-**1b** revealed completely analogous results to those described above: 2:2 mixed aggregates (*R*)-**15b** and (*S*)-**15b** formed exclusively in neat toluene or in toluene with low concentrations of THF, whereas (*R*)-**16b** and (*S*)-**16b** were the sole observable

Chart 3. Isomers of 3:1 Mixed Tetramer (*S*)-16a

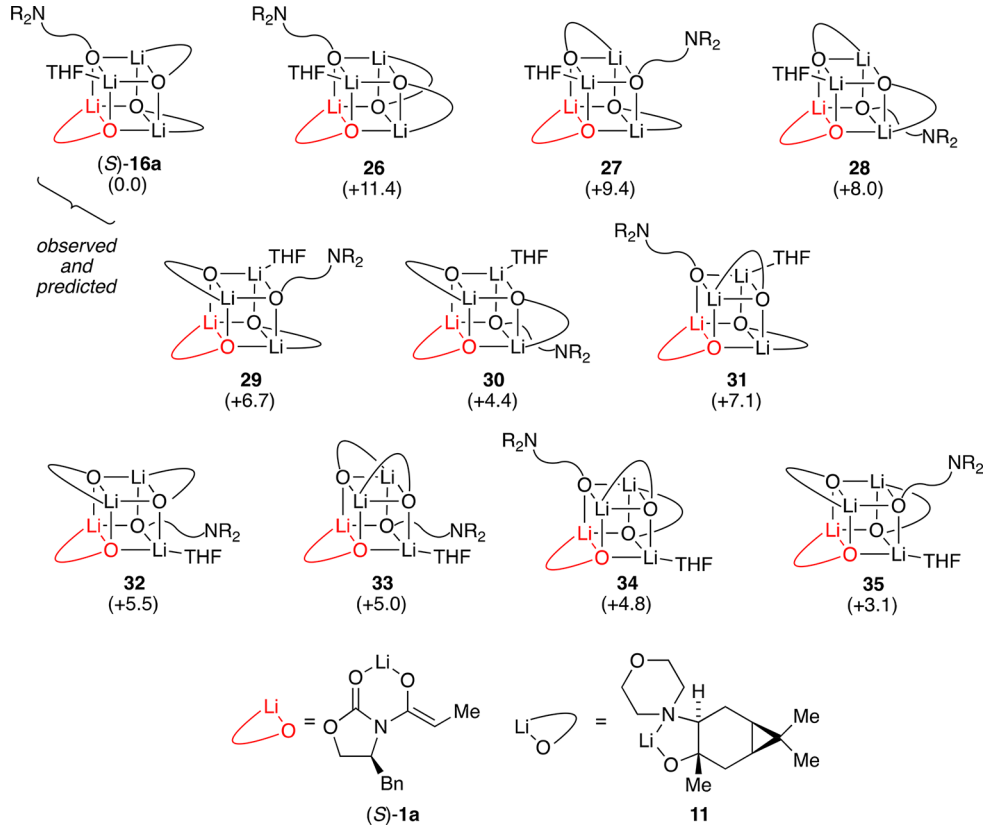

DOI: 10.1021/jacs.7b13776
J. Am. Chem. Soc. XXXX, XXX, XXX−XXX

mixed aggregates in neat THF. Differences in reactivity and selectivity are noted below.

Structures of Ephedrate-Derived Mixed Tetramers. The results of studies using ephedrate-derived alkoxide **8** showed notable departures from those obtained with the carane series. The valine-derived enolates, the **b** series, gave the cleanest results, and they are presented emblematically (Chart 4). Enolate-rich mixtures of enolate (*R*)-**1b** or (*S*)-**1b** and alkoxide **8** in *toluene* yielded no 1:3 (enolate-rich) mixed tetramer (see Figure 8B).

Chart 4. Mixed Aggregates Ephedrate 8 with (*S*)- and (*R*)-16a

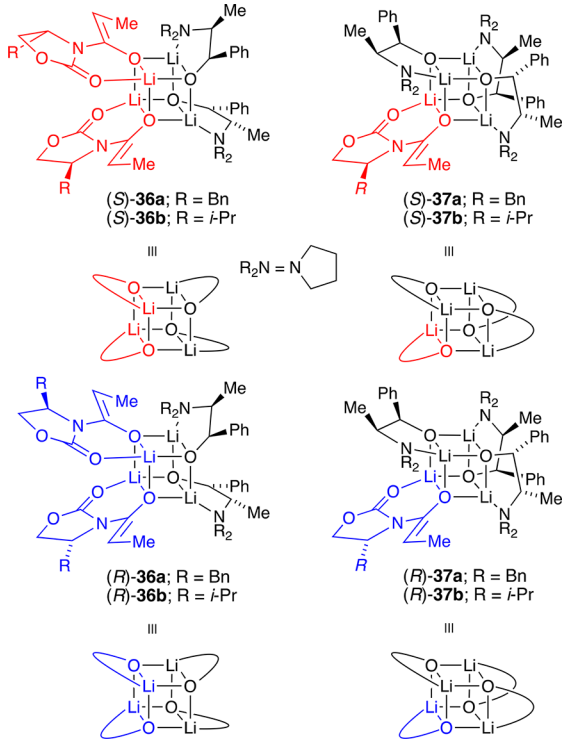

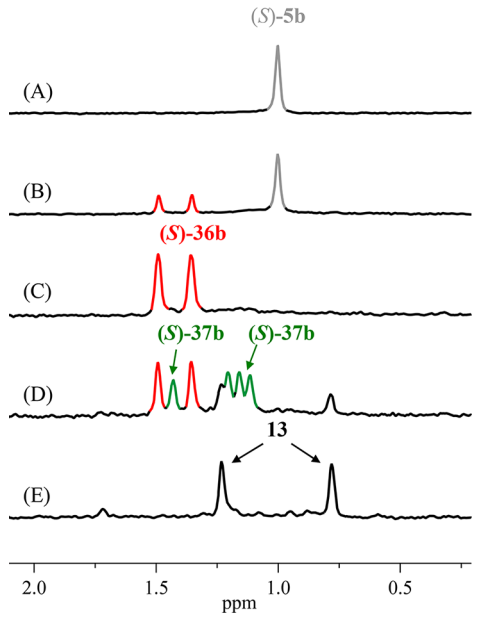

Figure 8. ^{6}Li NMR spectra of 0.10 M solutions of (*S*)-**1b** and alkoxide **8** in 0.11 M THF/toluene at −80 °C with 0.11 M [^{6}Li]LDA. The measured mole fractions[27] of alkoxide **8** (χ_{ROLi}) are 0.00, 0.18, 0.50, 0.69, and 1.00 for A–E, respectively.

Equimolar mixtures afforded 2:2 mixed tetramer (*S*)-**36b** or (*R*)-**36b** exclusively (see Figure 8C). Alkoxide-rich mixtures with enolate (*S*)-**1b** in neat THF afforded complex mixtures. In toluene, however, 3:1 mixed tetramer (*S*)-**37b** was produced as a single isomer, albeit *not* quantitatively (Figure 8D). Neither (*S*)-**36b** nor (*S*)-**37b** was influenced by added pyridine, which indicated that they are fully chelated. Mixed aggregate (*S*)-**36b** was characterized with the full complement of two-dimensional NMR spectroscopies (without ^{15}N labeling). Computations also supported the assignment of (*S*)-**36b** (Supporting Information). The stereochemistry of 3:1 mixed tetramer (*S*)-**37b**, by contrast, was tentatively distinguished from two other stereoisomers using only computations and should be viewed with some caution. Plotting aggregate concentration versus mole fraction of alkoxide **8** afforded a Job plot (Figure 9) that is almost unrecognizable

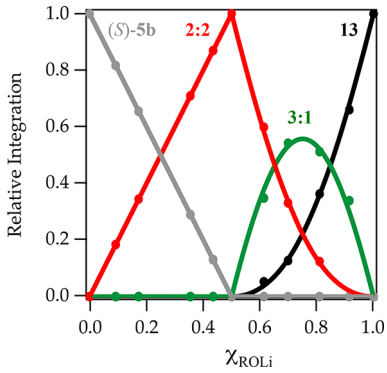

Figure 9. Job plot showing the relative integration of the ^{6}Li resonances versus the measured mole fraction[27] (χ_{ROLi}) of **8** at a 0.10 M constant total titer of (*S*)-**1b** and **8** in 0.11 M THF/toluene at −80 °C.

compared with the statistical analog (see Figure 3). The curves in Figures 3 and 9 both derive from the standard parametric fitting protocol used for any tetramer ensemble.

Table 1. Stereoselectivity of Aldol Additions Using Chiral Amino Alkoxides and Antipodes of Evans Enolates (Chart 5)[a]

entry	lithium alkoxide	aggregate	syn/syn (**2**/**38**)	syn/anti ([**2** + **38**]/**39**)	yield (%)
1	—	**3a**/**4a**	12:1	16:1	91
2	—	**5a**	1:1	5:1	<20
3	**11**	(*S*)-**15a**	6:1	7:1	54
4	**11**	(*R*)-**15a**	6:1	7:1	56
5	11	(*S*)-**16a**	**18:1**	**50:1**	**90**
6	11	(*R*)-**16a**	**2:1**	**5:1**	**88**
7	—	**3b**/**4b**	5:1	4:1	90
8	—	**5b**	1:5	3:1	<20
9	11	(*S*)-**15b**	**50:1**	**15:1**	**48**
10	11	(*R*)-**15b**	**50:1**	**14:1**	**45**
11	11	(*S*)-**16b**	**30:1**	**>100:1**	**92**
12	11	(*R*)-**16b**	**1:1**	**6:1**	**88**
13	**8**	(*S*)-**36a**	10:1	16:1	55
14	**8**	(*R*)-**36a**	10:1	14:1	50
15	**8**	(*S*)-**37a**	10:1	25:1	85
16	**8**	(*R*)-**37a**	10:1	8:1	78
17	**8**	(*S*)-**36b**	9:1	13:1	52
18	**8**	(*R*)-**36b**	9:1	13:1	55
19	**8**	(*S*)-**37b**	4:1	3:1	80
20	**8**	(*R*)-**37b**	9:1	4:1	79

[a]Reaction in neat tetrahydrofuran/−78 °C for 30 min *after* aging the enolate at 25 °C for 10 min; 2 equiv of electrophile.

DOI: 10.1021/jacs.7b13776
J. Am. Chem. Soc. XXXX, XXX, XXX−XXX

Chart 5. Aldol Adducts from Mixed Aggregates

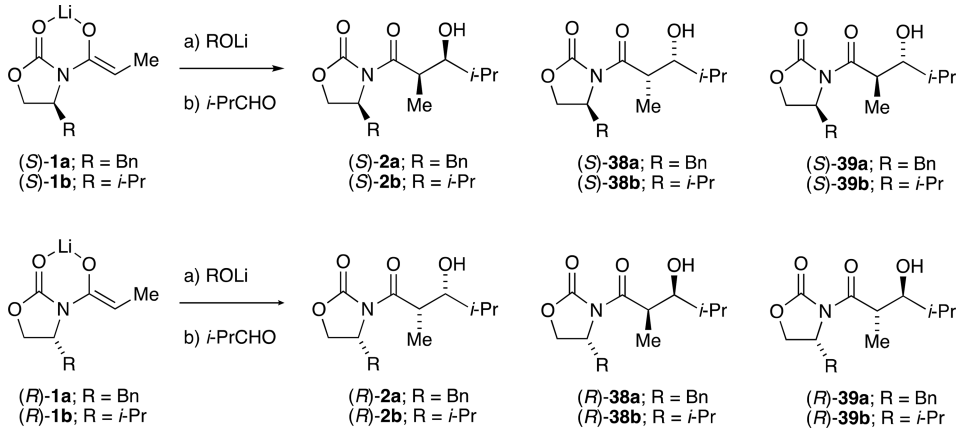

Equimolar mixtures of **8** and the phenylalanine-derived (*S*)-**1a** and (*R*)-**1a** enolates in toluene cleanly afforded fully characterized 2:2 mixed aggregates (*S*)-**36a** and (*R*)-**36a**. Alkoxide-rich mixtures in toluene afforded familiar patterns consistent with (*S*)-**37a** and (*R*)-**37a** along with other isomers. In neat THF, equimolar and alkoxide-rich samples afforded complex mixtures.

Aldol Additions: Stereoselectivity. Table 1 and Chart 5 summarize a number of aldol additions to *i*-PrCHO. The aggregate column lists the dominant aggregated form of enolates (*S*)-**1a**, (*R*)-**1a**, (*S*)-**1b**, or (*R*)-**1b** observed under the conditions of the aldol addition. (*S*) and (*R*) refer to the two antipodes of the Evans enolates that produce what are denoted "matched" and "mismatched" results. Entries 1−2 and 7−8 provide the results in the absence of amino alkoxide additives, as reported previously.[8] The poor results in entries 2 and 8 derive *not* from forcing conditions causing retroaldol additions, as described previously, but rather from slow partial conversion at −78 °C. The low (50%) yields in entries 13, 14, 17, and 18 stem from the stalling of the reaction after the consumption of one enolate subunit within the 2:2 mixed aggregates. Table 2 summarizes a limited survey of aldol selectivities (Scheme 5) using optimal 3:1 mixed aggregate (*S*)-**16b**.

Table 2. Stereoselectivity of Selected Aldol Additions

entry	RC(=O)R′	lithium alkoxide	syn/syn	syn/anti	yield (%)
1	PhC(=O)H[a]		1:3	1:12	70
2	PhC(=O)H[a]	**11**	>50:1	2:1	82
3	*t*-BuC(=O)H[b]		>50:1	>50:1	90
4	*t*-BuC(=O)H[b]	**11**	>50:1	>50:1	92
5	MeC(=O)CCH[b]		3:1	>50:1	80
6	MeC(=O)CCH[b]	**11**	7:1	>50:1	85
7	*i*-PrC(=O)Me				<5
8	*i*-PrC(=O)Me	**11**			<5

[a]Literature compound.[1b] [b]Characterized as described in the Supporting Information.

Aldol Additions: Rate Studies. Aside from the usual technical challenges of carrying out organolithium reaction kinetics, several acute problems arose during this study in particular. The rates of the aldol addition with *i*-PrCHO were too fast to monitor at −78 °C.[33] Given the choice of a lower temperature or a less reactive substrate, we turned to pivaldehyde (*t*-BuCHO; eq 6).

Rate studies under conditions favoring 2:2 mixed tetramer (*S*)-**15a** or (*S*)-**15b** were thwarted by odd (non-first-order) substrate losses and product formation. In contrast, the rate studies under conditions affording 3:1 mixed tetramer were far more satisfying. The existence of a single enolate subunit within the mixed aggregate may have helped. Monitoring the aldol addition by following the formation of aldolate (*S*)-**44a** (1788 cm^{-1}) rather than the embedded absorbance of *t*-BuCHO (1724 cm^{-1}) showed growth consistent with[34] pseudo-first-order behavior with aldehyde in deficiency and second-order behavior when the mixed aggregate and *t*-BuCHO were used in 1:1 proportions (Figure 10). Plotting pseudo-first-order rate constants (k_{obsd}) versus aldehyde concentration shows concentration-independent values of k_{obsd} (Figure 11), confirming the first-order dependence. Plotting k_{obsd} versus mixed aggregate concentration (Figure 12) and the concentration of *excess* alkoxide (Figure 13) shows approximate first-order and zeroth-order dependencies as expected (vide infra).

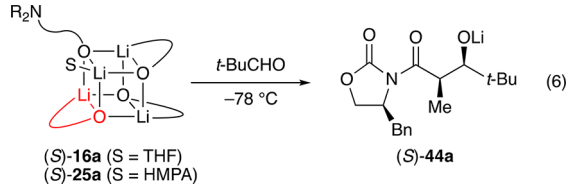

Determining the all-important reaction order in THF would require the monitoring of rates over a range of THF concentrations. However, even modest decreases in THF concentration from 12 M (neat THF) pushed the reactants from exclusive 3:1 mixed tetramer (*S*)-**15a** to the 2:2 mixed aggregates (eq 4), irreparably undermining the rate studies. Accordingly, we compromised yet again by using the isostructural HMPA solvate (*S*)-**25a**. The free (uncoordinated) HMPA concentration was varied over a 10-fold range (0.025−0.15 M) without a measurable change in structure. It was notable at the outset that, despite the enormous binding affinity of HMPA relative to THF,[35] the rates of additions in HMPA/toluene and neat THF were nearly indistinguishable. Despite the possibility of obtaining a number of uninformative outcomes that can result from the addition of such an invasive ligand, we obtained the one result that lent itself to literal interpretation unfettered by qualifiers: the reaction was zeroth-order in HMPA (Figure 14), which showed that the aldol proceeds via a mechanism that requires neither association nor dissociation of the sole coordinated solvent on the 3:1 mixed tetramer framework in the rate-limiting step. Using *t*-BuCDO afforded a k_H/k_D of 0.77 ± 0.016, which is consistent with a rate-limiting aldol addition. A rate-limiting complexation would afford a k_H/k_D of 1.0.

Altogether, the rate data implicate the idealized rate law[36,37] in eq 7 and the generic mechanism in eq 8, which are discussed

DOI: 10.1021/jacs.7b13776
J. Am. Chem. Soc. XXXX, XXX, XXX−XXX

Scheme 5. Aldol Additions to Various Aldehydes and Ketones Showing Amplification

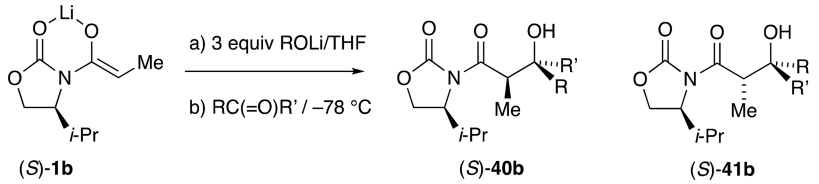

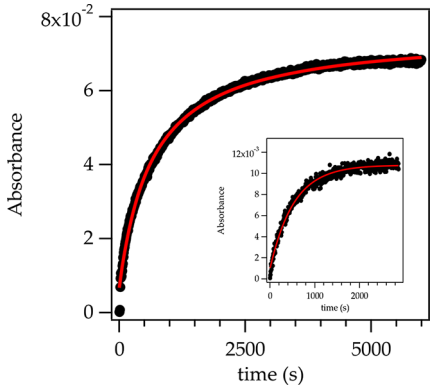

Figure 10. Formation of aldolate (*S*)-**44a** (1788 cm^{-1}) carried out using mixed tetramer (*S*)-**16a** (0.10 M) at −78 °C under second-order conditions [0.10 M pivaldehyde (*t*-BuCHO)] and pseudo-first-order conditions (0.010 M, inset). The curves represent fits to $f(x) = a - a/(1 + bx)$ and $f(x) = (a - 1)e^{-bx}$, respectively.

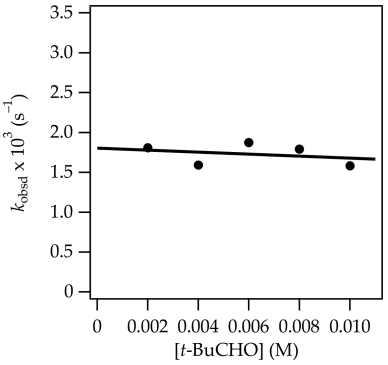

Figure 11. Plot of pseudo-first-order rate constants (k_{obsd}) versus *t*-BuCHO concentration in neat THF at −78 °C [0.10 M (*S*)-**16a**, neat THF]. The curve depicts an unweighted least-squares fit to the function $f(x) = ax + b$: $a = (-1.3 \pm 2.3) \times 10^{-2}$; $b = (2 \pm 2) \times 10^{-3}$.

below. We note here that the lack of deaggregation and solvent dissociation evidenced by the zeroth-order dependencies is critical.

$$d[P]/dt = k[RCHO][S]^0[(S)\text{-}\mathbf{16a}]^1[\mathbf{11}]^0 \quad (7)$$

$$(S)\text{-}\mathbf{16a} + RCHO \rightarrow [(S)\text{-}\mathbf{16a}]\cdot RCHO]^{\ddagger} \quad (8)$$

DISCUSSION

The work described herein falls into three categories: (1) characterization of ROLi−lithium enolate mixed tetramers; (2) development of stereoselective aldol additions of mixed tetramers; and (3) mechanistic study and determination of a stereochemical model for aldol addition.

Structures. The structural studies are summarized using the shorthand mnemonic described in Scheme 6 with color-coded loops for the *S* (red) and *R* (blue) enantiomeric series of Evans enolates. Detailed depictions of the tetrameric mixed aggregates

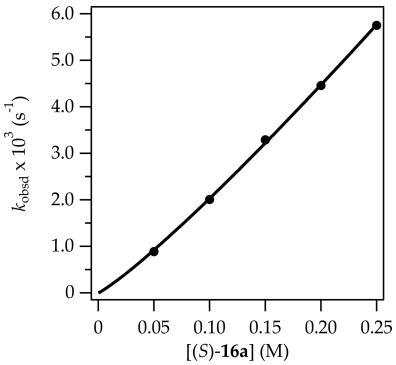

Figure 12. Plot of pseudo-first-order rate constants (k_{obsd}) versus (*S*)-**16a** concentration at 0.0050 M *t*-BuCHO in neat THF at −78 °C. The data were fit to $y = ax^n$ such that $n = 1.14 \pm 02$.

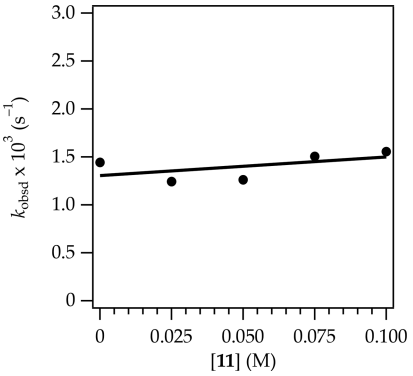

Figure 13. Plot of pseudo-first-order rate constants (k_{obsd}) versus the concentration of **11** in neat THF at −78 °C [0.10 M (*S*)-**16a**, neat THF]. The curve depicts an unweighted least-squares fit to the function $f(x) = ax + b$: $a = (1.94 \pm 1.8) \times 10^{-3}$; $b = (1.31 \pm 0.11) \times 10^{-3}$.

are found in Chart 1. The **a** and **b** series correspond to the phenylalanine- and valine-derived oxazolidinones, respectively. The characterizations required a range of tactics and strategies. Job plots show the gross aggregation states and stoichiometries of the mixed tetramers. Figure 9 offers the most unusual non-statistical example we have encountered to date. The presence or absence of chelation was confirmed with ^{15}N labeling of the amino alkoxide ([^{15}N]**11**). Coordination by external ligands was probed using pyridine as a ^{6}Li chemical shift reagent and HMPA to show specific solvent−lithium contacts through ^{6}Li−^{31}P coupling.[32] The stereochemical assignments stem from the application of a battery of two-dimensional spectroscopic methods complemented by DFT computations. Several mixed aggregates received less scrutiny but are secure nonetheless.

The various topologies of the D_{2d}-symmetric core of enolate tetramer **5** and the S_4-symmetric cores of alkoxide tetramers **13** and **14** conflict en route to the formation of mixed tetramers: the enolate topology dominates, but a structural mess was a distinct possibility. Alkoxides **8** and **11**, which form tetrameric cubes **13** and **14** (respectively), combine with both antipodes of

DOI: 10.1021/jacs.7b13776
J. Am. Chem. Soc. XXXX, XXX, XXX−XXX

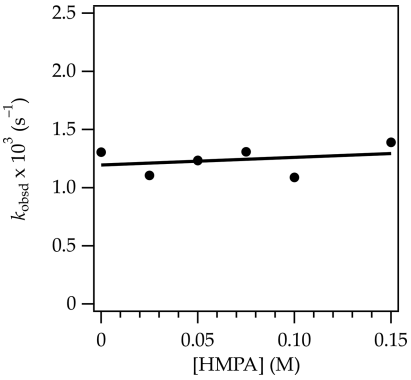

Figure 14. Plot of pseudo-first-order rate constants (k_{obsd}) versus hexamethylphosphoramide concentration in neat THF at −78 °C [0.10 M (*S*)-**16a**, neat THF]. The curve depicts an unweighted least-squares fit to the function $f(x) = ax + b$: $a = (6.4 \pm 10.6) \times 10^{-4}$; $b = (1.2 \pm 0.09) \times 10^{-3}$.

the Evans enolates—homotetramers (*S*)-**5a**, (*R*)-**5a**, (*S*)-**5b**, and (*R*)-**5b**—to form exclusively 2:2 mixed aggregates **15** *in toluene*, irrespective of stoichiometry. Mixtures containing excess alkoxide **11** cleanly afford (*S*)-**16** or (*R*)-**16** as a single stereoisomer but only in neat THF. The solvent concentration dependence can be traced to the preferential solvation of a single corner of the cube with accompanying scission of one of three amino alkoxide chelates. The stereocontrolled assembly of mixed tetramers **15** and **16** is remarkable given the enormous number of possible isomers (see Charts 2 and 3) consistent with the spectroscopic symmetries (many more if all possibilities are considered). Lithium enolates with excess ephedrate-derived alkoxide **8** received less scrutiny primarily because the structural control of the 3:1 mixed tetramers was poor. The absence of 1:3 enolate-rich mixed tetramers under any conditions is surprising, particularly given that (a) the enolate-like rather than alkoxide-like topologies of the resulting mixed aggregates dominate, and (b) simple enolates afford enolate-rich 1:3 mixed aggregates but not 3:1 alkoxide-rich mixed aggregates.

Stereoselective Aldol Additions. Our goal at the outset was to exploit amino alkoxide-containing mixed tetramers to amplify the inherent 12:1 (syn/syn) selectivity observed for aldol addition using lithiated Evans enolates (see Table 1, entry 1). Once again, we had numerous reasons for pessimism. The credible selectivity for unmodified Evans enolates was obtained from kinetically formed enolate dimers, which readily form fleeting monomers (see Scheme 2). The homotetrameric enolate **5** in THF formed by aging is decidedly unreactive, undergoing aldol addition via monomer stereorandomly and only under forcing conditions (see Table 1, entry 2). A glimmer of hope was found in contemporaneous studies of Weinreb enolates in which fully chelated tetramers showed evidence of coordinating external ligands to afford five-coordinate lithium owing to the geometric constraints of five-membered chelates.[22] We hoped the aldehyde might find its way into the mixed tetramer core.

We found two lines of evidence that mixed tetramers react without deaggregation: (1) the reactions were fast at −78 °C *even in neat toluene*, which contrasts with homotetramer **5**, and (2) the 2:2 mixed tetramers (**15**) markedly altered the stereoselectivity, albeit eroding the selectivity regardless of which enolate antipode was paired with alkoxide **11** (see Table 1, cf. entry 1 and entries 3 and 4). Fortunately, 3:1 mixed aggregates (*S*)-**16** and (*R*)-**16** showed the matched−mismatched influence we sought (Scheme 7). The *S* series (matched) amplified the aldol selectivity and eliminated low levels of the anti adduct (see Table 1, entries 5 and 11), whereas the *R* series (mismatched) eroded the selectivities (entries 6 and 12). When measured in kilocalories per mole, the stereochemical effects are small, but the measurable amplification is a satisfying proof of principle nonetheless. Ephedrate-derived alkoxide **8** showed inferior structural control and a lack of stereochemical influence (see Table 1, entries 13−20) that could be construed as evidence of a monomer-based aldol addition. That the aldol additions are fast at −78 °C does *not* exclude this possibility.

The optimized case, mixed tetramer (*S*)-**16b** derived from (*S*)-valine and alkoxide **11**, showed amplification of a few select aldol additions (see Table 2). This amplification is real but modest at best. The addition to benzaldehyde (entries 1 and 2) shows a mechanistically significant alkoxide-mediated reversal to produce synthetically unimportant overall stereoselectivity.

Stereochemical Model I: The Wrong One. We were tempted to invoke the THF-solvated lithium nucleus in 3:1 mixed tetramers (**16**) as the centerpiece of a stereochemical model (Scheme 8). Imagine the substitution of the lone THF by aldehyde which undergoes facile aldol addition via transition structure **46**. The first problem is that this aldol addition via (*S*)-**45a** predicts that the aldol should be (*S*)-**38a**, *the wrong product*. A simple corrective action is to assume equilibrium

Scheme 6. Summary of 2:2 and 3:1 Mixed Aggregates

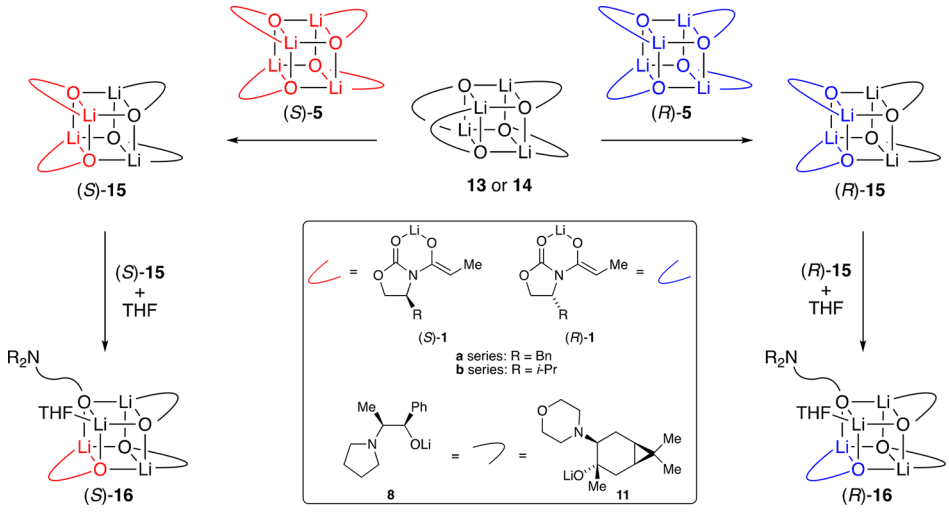

DOI: 10.1021/jacs.7b13776
J. Am. Chem. Soc. XXXX, XXX, XXX−XXX

Scheme 7. Stereoselectivity from Matched and Mismatched Enolate Antipodes (See Table 1)

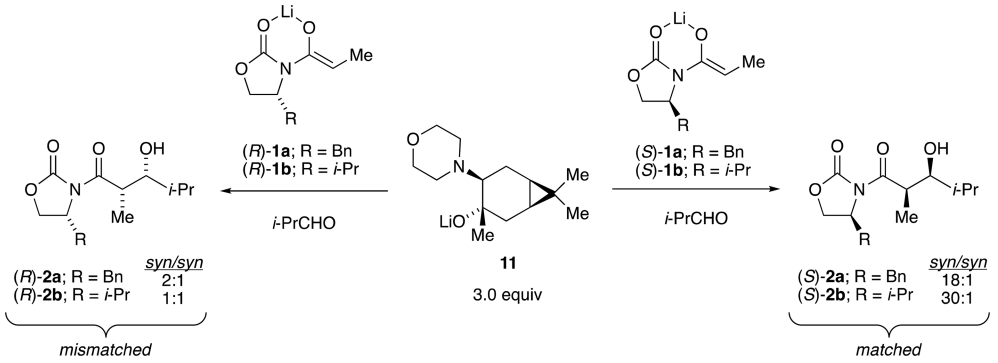

Scheme 8. Stereochemical Model I (Wrong)

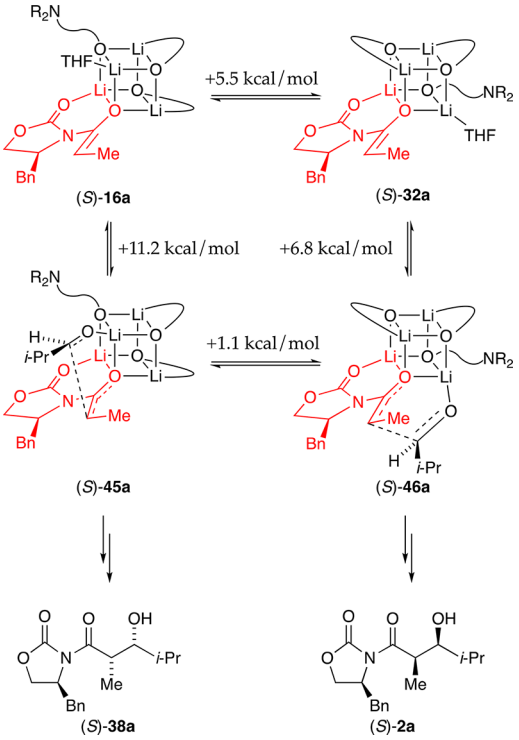

between observable mixed tetramer (*S*)-**16** and fleeting isomer (*S*)-**32a**, which is calculated to be 5.5 kcal/mol less stable. Substitution via aldehyde and aldol addition would give the correct aldol adduct **47** as the amplified form, a textbook example of the Curtin–Hammett principle. Alas, the computations predict transition structure (*S*)-**46a** to be less favorable than (*S*)-**45a**. In essence, the model incorrectly predicts an isomeric mismatch. This prediction is not a fundamental problem because computations can be wrong; we noted examples in the results section. A similar analysis using mixed tetramer (*R*)-**16a** derived from enolate (*R*)-**1a** should display amplified stereocontrol rather than the observed eroded (mismatched) stereoselectivity. The entire model is backward. There is, however, a more fundamental flaw.

Model I is pedagogically useful (easily envisioned) but incompatible with the rate data. To understand this incompatibility, we must digress. Detailed rate studies showed a first-order dependence on the less-reactive *t*-BuCHO and mixed tetramer (*S*)-**16a**. A zeroth-order dependence on alkoxide confirmed tetramer-based rather than monomer-based aldol addition. Had the reaction proceeded via monomer-based transition structure **6** (see Scheme 2), the rate law would reflect the dissociation of the three alkoxide subunits (eq 9) as *inverse three-fourths order* in alkoxide **11**. However, a zeroth-order was observed. Moreover, substituting the coordinated THF on mixed tetramer **16** with a strongly bound HMPA should inhibit a reaction requiring the substitution of the coordinated solvent: HMPA demonstrably

$$\underset{(S)\text{-}\mathbf{16a}}{(\text{enolate})(\text{ROLi})_3(\text{S})} + \text{S} \not\rightleftharpoons (\text{enolate})\text{S}_2 + 3/4(\underset{\mathbf{14}}{\text{ROLi})_4} \quad (9)$$

$$\underset{(S)\text{-}\mathbf{16a}}{(\text{enolate})(\text{ROLi})_3(\text{S})} + \text{RCHO} \not\rightleftharpoons (\text{enolate})(\text{ROLi})_3(\text{RCHO}) + \text{S} \quad (10)$$

binds but imparts *no* detectable change in reaction rate or stereochemistry. An affiliated zeroth-order in solvent (HMPA in the rate studies) shows that the solvent is *not* substituted by the aldehyde en route to the aldol addition. Model I is fatally flawed.

Stereochemical Model II: The Right One? The nondissociative pathway mandated by the rate studies requires that (*S*)-**16a** react either directly using an ill-defined coordination site or via chelate scission. Although spectroscopic and computational studies of Weinreb amides suggest that five-membered chelates leave open the possibility of trigonal–bipyramidal (five-coordinate) lithiums on cubic tetramers,[22] computational evidence lends no support for a five-coordinate lithium in the highly congested 3:1 mixed tetramer (*S*)-**16**. Instead, we invoke a *second* chelate scission with aldehyde coordination (Scheme 9).

Model II correctly predicts amplification in the *S* series (matched) and eroded selectivities in the *R* series (mismatched). The absolute activation energies of model II are comparable to those in model I for both the matched and mismatched pairings. We must confess to having had no clue at the outset that our preferred model would involve a monochelated mixed tetramer, which is somewhat disruptive to our thinking in that more tightly bound (fully chelated) mixed aggregates would be potentially more predictive and possibly impart even greater selectivity.

Stereochemically Enigmatic 2:2 Mixed Tetramers. The story took a huge detour when we investigated the influence of 2:2 mixed tetramers. Members of the phenylalanine-derived **a** series were poorly selective regardless of the choice of enantiomeric pairing of (*R*)-**15a** or (*S*)-**15a**, *but there was no evidence of match–mismatch pairing.* Valine-derived (*S*)-**15b** and (*R*)-**15b** also react rapidly at −78 °C. Yields of approximately 50% can be traced to stalling after the consumption of one of the two enolate subunits. Remarkably, (*R*)-**15b** and (*S*)-**15b** elicit strikingly amplified selectivities, affording 50:1 syn/syn selectivities accompanied by low levels of one anti isomer (eq 11). Moreover, *the aldol selectivities are independent of the enantiomeric pairings.* The conundrum is that mixed aggregates (*R*)-**15b** and (*S*)-**15b** promote highly selective alkylation from the face oppo-

DOI: 10.1021/jacs.7b13776
J. Am. Chem. Soc. XXXX, XXX, XXX–XXX

Scheme 9. Stereochemical Model II Showing Matched and Mismatched Selectivities

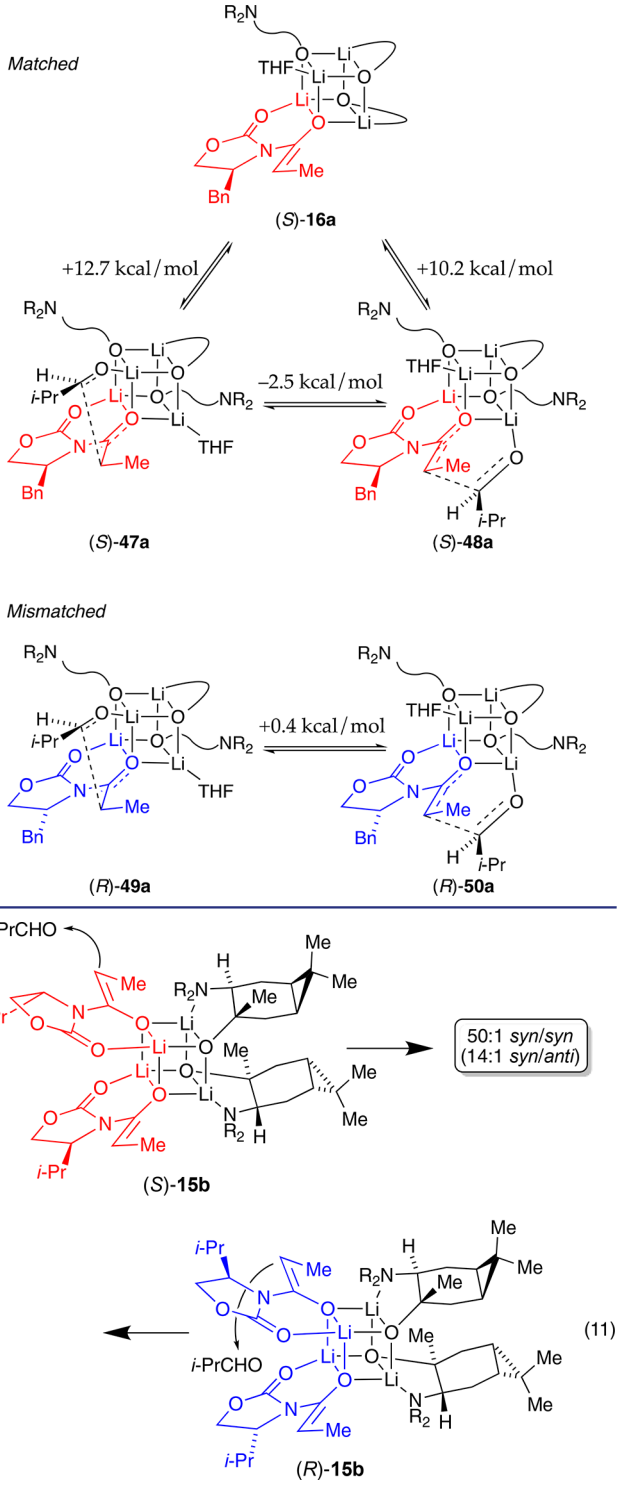

site the isopropyl substituent despite strikingly complementary trajectories. The absence of mechanistic data owing to odd curvatures would not stop us from proposing a stereochemical model, but we do not have a particularly satisfying one.

The amplification regardless of chiral pairing—that both aggregates act as matched—suggests that the influence of the alkoxide auxiliaries specific to the 2:2 mixed aggregates has nothing to do with chirality. This conclusion prompted a last series of experiments. Equimolar mixtures of achiral alkoxide **51** and enolate (*S*)-**1b** cleanly afforded a single 2:2 mixed aggregate shown by the full complement of NMR spectroscopies to be **52**. The preference for **52** with the isopropyl moieties proximate to each other

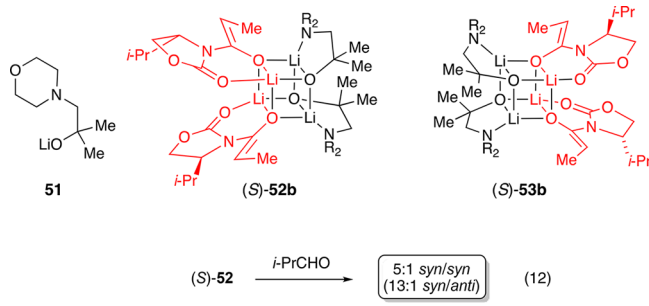

rather than **53** with the isopropyl moieties proximate to the alkoxides shows an inherent preference uninfluenced by relative alkoxide stereochemistry. We did indeed modify the selectivity (eq 12) but not favorably.

CONCLUSIONS

Our effort to exploit the DuPont and Merck chiral amino alkoxides to impart stereocontrol of enolate reactions is a good proof of principle. Controlling 2:2 and 3:1 mixed tetramer structures and achieving direct reaction without intervening deaggregations are considerable steps. Evidence of matched and mismatched modified selectivities for an aldol addition confirms that we can control selectivity through aggregate structures. It goes without saying that 100:1 selectivities would have been great, but the proof of principle is clear. Our wish list, however, is extensive. Reversing the enolate configuration rather than the alkoxide configuration nicely illustrates the matching and mismatching of chiral subunits but has obvious limitations in a goal to *control* stereochemistry. An amino alkoxide for which both antipodes are readily available is important. This problem is familiar to those who work with sparteine as a chiral ligand.[38] Surprisingly, the 2:2 mixed aggregates show considerable amplification that was fully independent of the relative chiralities of the subunits. This outcome, in theory, solves the chirality problem for the specific study in question, but it begs a fundamental question: How?

We had the notion that 2:2 mixed aggregates could offer a remarkably simple, albeit ironic, solution by amplifying selectivities using *achiral* alkoxides—elaborate lithium chloride surrogates if you will. The idea that using even simple achiral amino alkoxides to modify organolithium reactivity has been exploited most notably by Caubère.[39] That these achiral compounds could influence stereocontrol is a provocative idea that has been validated: selectivities were amplified, but in a single attempt, the effects were small. There is room for improvement.

Of course, imparting 99% stereoselectivity on reactions of achiral chelating enolates, whether oxazolidinone-based or not, would be a considerable advance. In the long run, however, a universal alkoxide available in both antipodes that can *amplify* stereoselectivity in a range of chelating enolates would also be meritorious and attainable.

EXPERIMENTAL SECTION

Reagents and Solvents. THF, toluene, and pyridine were distilled from solutions containing sodium benzophenone ketyl. LDA, [^{6}Li]LDA, [^{6}Li,^{15}N]LDA, lithium hexamethyldisilazide (LiHMDS), [^{6}Li]-LiHMDS, and [^{6}Li,^{15}N]LiHMDS were prepared as described previously. Solutions of LDA and LiHMDS were titrated for active base by using a literature method.[40] Air- and moisture-sensitive materials

DOI: 10.1021/jacs.7b13776
J. Am. Chem. Soc. XXXX, XXX, XXX−XXX

were manipulated under argon using standard glovebox, vacuum line, and syringe techniques. The Evans enolate precursors were purchased, and amino alcohols were obtained from Merck and Bristol-Myers Squibb (formerly DuPont Pharmaceuticals).

NMR Spectroscopy. Individual stock solutions of substrates and LDA or LiHMDS were prepared at room temperature. An NMR tube under vacuum was flame-dried on a Schlenk line and allowed to return to room temperature. It was then backfilled with argon and placed in a −78 °C dry ice/acetone bath. Appropriate amounts of LDA or LiHMDS (1.1 equiv), amino alcohol, and oxazolidinone enolate were added sequentially via syringe. The tubes were sealed under partial vacuum and vortexed on a vortex mixer for 5 s. They could then be stored for days in a freezer at −86 °C. Each sample routinely contained 0.10 M total substrate with a 0.01 M excess of LDA or LiHMDS. (The excess base could not be observed in samples after aging as shown by ^{6}Li and ^{15}N NMR spectroscopies.) Standard ^{6}Li and ^{13}C NMR spectra were recorded on a 500 MHz spectrometer at 73.57 and 125.79 MHz, respectively. The ^{6}Li resonances were referenced to 0.30 M [^{6}Li]LiCl/methanol at −80 °C (0.0 ppm).

IR Spectroscopic Analyses. IR spectra were recorded with an in situ IR spectrometer fitted with a 30-bounce, silicon-tipped probe. The spectra were acquired in 16 scans at a gain of 1 and a resolution of 4 cm^{-1}. A representative reaction was carried out as follows: The IR probe was inserted through a nylon adapter and O-ring seal into an oven-dried, cylindrical flask fitted with a magnetic stir bar and a T-joint. The T-joint was capped with a septum for injections and a nitrogen line. After evacuation under full vacuum, heating, and flushing with nitrogen, the flask was charged with LDA (56 mg, 0.525 mmol) or LiHMDS (88 mg, 0.525 mmol) in THF, cooled in a dry ice/acetone bath prepared with fresh acetone, and charged with (*S*)-**1a** (29 mg, 0.25 mmol) and **11** (90 mg, 0.75 mmol) in THF. The total volume was brought to 4.9 mL with THF. After a background spectrum was recorded, *t*-BuCHO (0.050 mmol) as a 0.25 M stock solution in THF was added with stirring. IR spectra were recorded every 6 s with monitoring of the absorbance at 1788 cm^{-1} over the course of the reaction.

Preparative-Scale Addition of *i*-PrCHO. LiHMDS (4.11 g, 24.6 mmol) was weighed out in a 100 mL round-bottom flask inside a glovebox, and the flask was sealed with a septum. After the flask was transferred outside the glovebox, the lithium base was dissolved in 40 mL of freshly distilled THF. The solution was cooled to −78 °C in a dry ice/acetone bath. A mixture of (*S*)-**1b** (1.11 g, 6.0 mmol) and **11** (4.43 g, 18.5 mmol) in 20 mL of THF was added dropwise to the cooled solution. The mixture was warmed to 25 °C for 10 min, recooled to −78 °C, and allowed to stir for 15 min. Then, 1.10 mL of freshly distilled *i*-PrCHO (0.87 g, 12.0 mmol) in 2.0 mL of THF was added to the reaction mixture. After 30 min of stirring at −78 °C, the reaction was quenched with 10 mL concentrated HCl. The solution was warmed to room temperature and extracted with three 100 mL portions of diethyl ether. The organic extracts were washed with 100 mL brine, dried over sodium sulfate, and concentrated in vacuo. The crude product was analyzed with ^{1}H and ^{13}C NMR. After flash chromatography with 20% ethyl acetate in hexanes, 1.42 g of product was obtained (92% yield). (*S*)-**2b**: ^{1}H NMR (599 MHz, $CDCl_3$) δ 4.43 (ddd, J = 8.4, 4.0, 3.1 Hz, 1H), 4.25 (dd, J = 9.2, 8.4 Hz, 1H), 4.18 (dd, J = 9.2, 3.1 Hz, 1H), 4.03 (qd, J = 7.0, 3.2 Hz, 1H), 3.53 (dd, J = 8.2, 3.2 Hz, 1H), 2.45 (s, 1H), 2.31 (ddq, J = 10.9, 6.9, 3.9, 3.5 Hz, 1H), 1.67 (dp, J = 8.2, 6.7 Hz, 1H), 1.11 (d, J = 7.0 Hz, 3H), 0.99 (d, J = 6.6 Hz, 3H), 0.90 (d, J = 6.8 Hz, 3H), 0.88 (d, J = 7.0 Hz, 3H), 0.85 (d, J = 6.9 Hz, 3H). ^{13}C NMR (126 MHz, $CDCl_3$) δ 177.4, 153.7, 77.2, 63.3, 58.5, 39.9, 31.2, 28.5, 19.1, 19.0, 18.0, 14.7, 9.8. Direct analysis in real-time mass spectrometry m/z calcd for $C_{13}H_{22}NO_3$ $(M + H - H_2O)^+$ 240.15942, found 240.15923. The minor isomers were observed using NMR spectroscopy with comparison to independently prepared authentic samples (Supporting Information).

■ ASSOCIATED CONTENT

Supporting Information

The Supporting Information is available free of charge on the ACS Publications website at DOI: 10.1021/jacs.7b13776.

Video discussing the experimental process (MOV)
Video discussing the experimental process (MOV)
Video discussing the experimental process (MOV)
NMR spectroscopic, kinetic, and computational data (PDF)

■ AUTHOR INFORMATION

Corresponding Author

*dbc6@cornell.edu

ORCID

David B. Collum: 0000-0001-6065-1655

Notes

The authors declare no competing financial interest.

■ ACKNOWLEDGMENTS

We thank the National Institutes of Health (GM077167) for support.

■ REFERENCES

(1) (a) Evans, D. A.; Bartroli, J.; Shih, T. L. *J. Am. Chem. Soc.* **1981**, *103*, 2127. (b) Evans, D. A.; Takacs, J. M.; McGee, L. R.; Ennis, M. D.; Mathre, D. J.; Bartroli, J. *Pure Appl. Chem.* **1981**, *53*, 1109.

(2) (a) Ager, D. J.; Prakash, I.; Schaad, D. R. *Chem. Rev.* **1996**, *96*, 835. (b) Wu, G.; Huang, M. *Chem. Rev.* **2006**, *106*, 2596. (c) Farina, V.; Reeves, J. T.; Senanayake, C. H.; Song, J. J. *Chem. Rev.* **2006**, *106*, 2734. (d) Evans, D. A.; Shaw, J. T. *Lactualité Chim.* **2003**, 35. (e) Lin, G.-Q.; Li, Y.-M.; Chan, A. S. C. *Principles and Applications of Asymmetric Synthesis*; Wiley & Sons: New York, 2001; p 135. (f) Ager, D. J.; Prakash, I.; Schaad, D. R. *Aldrichimica Acta* **1997**, *30*, 3.

(3) (a) Evans, D. A.; Ennis, M. D.; Mathre, D. J. *J. Am. Chem. Soc.* **1982**, *104*, 1737. (b) Kitajima, H.; Nakamura, M.; Tamakawa, H.; Goto, N. *Bioorg. Med. Chem. Lett.* **2000**, *10*, 2453. (c) Bull, S. D.; Davies, S. G.; Nicholson, R. L.; Sanganee, H. J.; Smith, A. D. *Org. Biomol. Chem.* **2003**, *1*, 2886. (d) Hara, A.; Morimoto, R.; Ishikawa, Y.; Nishiyama, S. *Org. Lett.* **2011**, *13*, 4036. (e) Li, L.; Ding, J.; Gao, L.; Han, F. *Org. Biomol. Chem.* **2015**, *13*, 1133.

(4) (a) Evans, D. A.; Wu, L. D.; Wiener, J. J. M.; Johnson, J. S.; Ripin, D. H. B.; Tedrow, J. S. *J. Org. Chem.* **1999**, *64*, 6411. (b) Crimmins, M. T.; Emmitte, K. A.; Katz, J. D. *Org. Lett.* **2000**, *2*, 2165. (c) Cases, M.; Gonzalez-Lopez de Turiso, F.; Hadjisoteriou, M. S.; Pattenden, G. *Org. Biomol. Chem.* **2005**, *3*, 2786. (d) Green, R.; Merritt, A. T.; Bull, S. D. *Chem. Commun.* **2008**, 508. (e) McLeod, M. C.; Wilson, Z. E.; Brimble, M. A. *J. Org. Chem.* **2012**, *77*, 400.

(5) (a) *Modern Aldol Reactions*; Mahrwald, R., Ed.; Wiley-VCH: Weinheim, 2004; Vols. 1 and 2. (b) Palomo, C.; Oiarbide, M.; Garcia, J. M. *Chem. Soc. Rev.* **2004**, *33*, 65. (c) Franklin, A. S.; Paterson, I. *Contemp. Org. Synth.* **1994**, *1*, 317. (d) Baiget, J.; Cosp, A.; Galvez, E.; Gomez-Pinal, L.; Romea, P.; Urpi, F. *Tetrahedron* **2008**, *64*, 5637. (e) Velazquez, F.; Olivo, H. *Curr. Org. Chem.* **2002**, *6*, 303.

(6) (a) Singer, R. A.; Ragan, J. A.; Bowles, P.; Chisowa, E.; Conway, B. G.; Cordi, E. M.; Leeman, K. R.; Letendre, L. J.; Sieser, J. E.; Sluggett, G. W.; Stanchina, C. L.; Strohmeyer, H.; Blunt, J.; Taylor, S.; Byrne, C.; Lynch, D.; Mullane, S.; O'Sullivan, M. M.; Whelan, M. *Org. Process Res. Dev.* **2014**, *18*, 26. (b) Fürstner, A.; Bouchez, L. C.; Morency, L.; Funel, J.; Liepins, V.; Porée, F.; Gilmour, R.; Laurich, D.; Beaufils, F.; Tamiya, M. *Chem. - Eur. J.* **2009**, *15*, 3983. (c) Theurer, M.; Fischer, P.; Baro, A.; Nguyen, G. S.; Kourist, R.; Bornscheuer, U.; Laschat, S. *Tetrahedron* **2010**, *66*, 3814. (d) Peters, R.; Althaus, M.; Diolez, C.; Rolland, A.; Manginot, E.; Veyrat, M. *J. Org. Chem.* **2006**, *71*, 7583. (e) Liu, W.; Sheppeck, J. E., II; Colby, D. A.; Huang, H.; Nairn, A. C.; Chamberlin, A. R. *Bioorg. Med. Chem. Lett.* **2003**, *13*, 1597. (f) Ojida, A.; Yamano, T.; Taya, N.; Tasaka, A. *Org. Lett.* **2002**, *4*, 3051. (g) Bartroli, J.; Turmo, E.; Belloc, J.; Forn, J. *J. Org. Chem.* **1995**, *60*, 3000.

(7) (a) Sobahi, T. R. *Orient. J. Chem.* **2004**, *20*, 17. (b) Bonner, M. P.; Thornton, E. R. *J. Am. Chem. Soc.* **1991**, *113*, 1299. (c) Pridgen, L. N.; Abdel-Magid, A. F.; Lantos, I.; Shilcrat, S.; Eggleston, D. S. *J. Org. Chem.* **1993**, *58*, 5107. (d) Abdel-Magid, A.; Pridgen, L. N.; Eggleston, D. S.; Lantos, I. *J. Am. Chem. Soc.* **1986**, *108*, 4595. (e) Pridgen, L. N.; Abdel-

DOI: 10.1021/jacs.7b13776
J. Am. Chem. Soc. XXXX, XXX, XXX−XXX

Magid, A.; Lantos, I. *Tetrahedron Lett.* **1989**, *30*, 5539. (f) Banks, M. R.; Blake, A. J.; Cadogan, J. I. G.; Dawson, I. M.; Gaur, S.; Gosney, I.; Gould, R. O.; Grant, K. J.; Hodgson, P. K. G. *J. Chem. Soc., Chem. Commun.* **1993**, 1146. (g) Xue, C.; Voss, M. E.; Nelson, D. J.; Duan, J. J. W.; Cherney, R. J.; Jacobson, I. C.; He, X.; Roderick, J.; Chen, L.; Corbett, R. L.; Wang, L.; Meyer, D. T.; Kennedy, K.; DeGrado, W. F.; Hardman, K. D.; Teleha, C. A.; Jaffee, B. D.; Liu, R.; Copeland, R. A.; Covington, M. B.; Christ, D. D.; Trzaskos, J. M.; Newton, R. C.; Magolda, R. L.; Wexler, R. R.; Decicco, C. P. *J. Med. Chem.* **2001**, *44*, 2636. (h) Jacobson, I. C.; Reddy, G. P. *Tetrahedron Lett.* **1996**, *37*, 8263.

(8) Tallmadge, E. H.; Jermaks, J.; Collum, D. B. *J. Am. Chem. Soc.* **2016**, *138*, 345.

(9) Tallmadge, E. H.; Collum, D. B. *J. Am. Chem. Soc.* **2015**, *137*, 13087.

(10) March, J. *Advanced Organic Chemistry*, 4th ed.; Wiley: New York, 1980; p 959.

(11) (a) Seebach, D. *Angew. Chem., Int. Ed. Engl.* **1988**, *27*, 1624. (b) Seebach, D. In *Proceedings of the Robert A. Welch Foundation Conferences on Chemistry and Biochemistry*; Wiley: New York, 1984; p 93.

(12) For reviews of structures and reactivities of organolithium mixed aggregates, see: Harrison-Marchand, A.; Mongin, F. *Chem. Rev.* **2013**, *113*, 7470. Luderer, M. R.; Bailey, W. F.; Luderer, M. R.; Fair, J. D.; Dancer, R. J.; Sommer, M. B. *Tetrahedron: Asymmetry* **2009**, *20*, 981.

(13) (a) Grabowski, E. J. J. Reflections on Process Research. In *Chemical Process Research: The Art of Practical Organic Synthesis*; Abdel-Magid, A. F., Ragan, J. A., Eds.; American Chemical Society: Washington DC, 2004; pp 1−21. (b) Huffman, M. A.; Yasuda, N.; DeCamp, A. E.; Grabowski, E. J. J. *J. Org. Chem.* **1995**, *60*, 1590. (c) Grabowski, E. J. J. *Chirality* **2005**, *17*, S249.

(14) (a) Thompson, A.; Corley, E. G.; Huntington, M. F.; Grabowski, E. J. J.; Remenar, J. F.; Collum, D. B. *J. Am. Chem. Soc.* **1998**, *120*, 2028. (b) Xu, F.; Reamer, R. A.; Tillyer, R.; Cummins, J. M.; Grabowski, E. J. J.; Reider, P. J.; Collum, D. B.; Huffman, J. C. *J. Am. Chem. Soc.* **2000**, *122*, 11212. (c) Thompson, A. S.; Corley, E. G.; Huntington, M. F.; Grabowski, E. J. J. *Tetrahedron Lett.* **1995**, *36*, 8937.

(15) (a) Pierce, M. E.; Parsons, R. L., Jr.; Radesca, L. A.; Lo, Y. S.; Silverman, S.; Moore, J. R.; Islam, Q.; Choudhury, A.; Fortunak, J. M. D.; Nguyen, D.; Luo, C.; Morgan, S. J.; Davis, W. P.; Confalone, P. N.; Chen, C. Y.; Tillyer, R. D.; Frey, L.; Tan, L. S.; Xu, F.; Zhao, D.; Thompson, A. S.; Corley, E. G.; Grabowski, E. J. J.; Reamer, R.; Reider, P. J. *J. Org. Chem.* **1998**, *63*, 8536. (b) Huffman, M. A.; Yasuda, N.; DeCamp, A. E.; Grabowski, E. J. J. *J. Org. Chem.* **1995**, *60*, 1590. (c) Kauffman, G. S.; Harris, G. D.; Dorow, R. L.; Stone, B. R. P.; Parsons, R. L., Jr.; Pesti, J. A.; Magnus, N. A.; Fortunak, J. M.; Confalone, P. N.; Nugent, W. A. *Org. Lett.* **2000**, *2*, 3119.

(16) (a) Parsons, R. L., Jr.; Fortunak, J. M.; Dorow, R. L.; Harris, G. D.; Kauffman, G. S.; Nugent, W. A.; Winemiller, M. D.; Briggs, T. F.; Xiang, B.; Collum, D. B. *J. Am. Chem. Soc.* **2001**, *123*, 9135. (b) Briggs, T. F.; Winemiller, M. D.; Collum, D. B.; Parsons, R. L., Jr.; Davulcu, A. K.; Harris, G. D.; Fortunak, J. D.; Confalone, P. N. *J. Am. Chem. Soc.* **2004**, *126*, 5427. (c) Sun, X.; Winemiller, M. D.; Xiang, B.; Collum, D. B. *J. Am. Chem. Soc.* **2001**, *123*, 8039.

(17) Parsons, R. L., Jr. *Curr. Opin. Drug Discovery Dev.* **2000**, *3*, 783.

(18) Bruneau, A. M.; Liou, L.; Collum, D. B. *J. Am. Chem. Soc.* **2014**, *136*, 2885.

(19) For a review on aggregation and cooperative effects on the aldol additions of lithium enolates, see: Larranaga, O.; de Cozar, A.; Bickelhaupt, F. M.; Zangi, R.; Cossio, F. P. *Chem. - Eur. J.* **2013**, *19*, 13761.

(20) Renny, J. S.; Tomasevich, L. L.; Tallmadge, E. H.; Collum, D. B. *Angew. Chem., Int. Ed.* **2013**, *52*, 11998.

(21) Job, P. *Ann. Chim.* **1928**, *9*, 113.

(22) (a) Liou, L. R.; McNeil, A. J.; Ramírez, A.; Toombes, G. E. S.; Gruver, J. M.; Collum, D. B. *J. Am. Chem. Soc.* **2008**, *130*, 4859. (b) Houghton, M. J.; Collum, D. B. *J. Org. Chem.* **2016**, *81*, 11057.

(23) After surveying a subset of the community, we have chosen to refer to $(LiX)_n$ and $(LiX)_m(LiX')_n$ as "homoaggregate" and "heteroaggregate," respectively, and reserve the term "mixed aggregate" for $(LiX)_m(LiY)_n$.

(24) (a) Friebolin, H. *Basic One- and Two-Dimensional NMR Spectroscopy*; Wiley VCH: Weinheim, 2010. (b) Claridge, T. D. W. *High-Resolution NMR Techniques in Organic Chemistry*, 2nd ed.; Elsevier: Amsterdam, 2009.

(25) *Gaussian 09*, Revision A.02: Frisch, M. J.; Trucks, G. W.; Schlegel, H. B.; Scuseria, G. E.; Robb, M. A.; Cheeseman, J. R.; Scalmani, G.; Barone, V.; Petersson, G. A.; Nakatsuji, H.; Li, X.; Caricato, M.; Marenich, A.; Bloino, J.; Janesko, B. G.; Gomperts, R.; Mennucci, B.; Hratchian, H. P.; Ortiz, J. V.; Izmaylov, A. F.; Sonnenberg, J. L.; Williams-Young, D.; Ding, F.; Lipparini, F.; Egidi, F.; Goings, J.; Peng, B.; Petrone, A.; Henderson, T.; Ranasinghe, D.; Zakrzewski, V. G.; Gao, J.; Rega, N.; Zheng, G.; Liang, W.; Hada, M.; Ehara, M.; Toyota, K.; Fukuda, R.; Hasegawa, J.; Ishida, M.; Nakajima, T.; Honda, Y.; Kitao, O.; Nakai, H.; Vreven, T.; Throssell, K.; Montgomery, J. A., Jr.; Peralta, J. E.; Ogliaro, F.; Bearpark, M.; Heyd, J. J.; Brothers, E.; Kudin, K. N.; Staroverov, V. N.; Keith, T.; Kobayashi, R.; Normand, J.; Raghavachari, K.; Rendell, A.; Burant, J. C.; Iyengar, S. S.; Tomasi, J.; Cossi, M.; Millam, J. M.; Klene, M.; Adamo, C.; Cammi, R.; Ochterski, J. W.; Martin, R. L.; Morokuma, K.; Farkas, O.; Foresman, J. B.; Fox, D. J. Gaussian, Inc., Wallingford, CT, 2016.

(26) Phenomena such as "memory of chirality" could owe their selectivity to slow aggregate exchange: Kawabata, T.; Fuji, K. *Topics in Stereochemistry* **2003**, *23*, 175.

(27) The measured mole fraction, the mole fraction within only the ensemble of interest, rather than the intended mole fraction of the enolates added to the samples eliminates the distorting effects of impurities.

(28) For an example and leading references to the influence of aromatic hydrocarbons on organolithium structures and reactivities, see: Reyes-Rodríguez, G. J.; Algera, R. F.; Collum, D. B. *J. Am. Chem. Soc.* **2017**, *139*, 1233.

(29) Jackman and co-workers described extensive studies of phenolates in pyridine.[30]

(30) (a) Jackman, L. M.; DeBrosse, C. W. *J. Am. Chem. Soc.* **1983**, *105*, 4177. (b) Jackman, L. M.; Smith, B. D. *J. Am. Chem. Soc.* **1988**, *110*, 3829. (c) Jackman, L. M.; Chen, X. *J. Am. Chem. Soc.* **1997**, *119*, 8681. (d) Jackman, L. M.; Petrei, M. M.; Smith, B. D. *J. Am. Chem. Soc.* **1991**, *113*, 3451.

(31) (a) MacDougall, D. J.; Noll, B. C.; Kennedy, A. R.; Henderson, K. W. *J. Chem. Soc., Dalton Trans.* **2006**, *15*, 1875. (b) Boyle, T. J.; Pedrotty, D. M.; Alam, T. M.; Vick, S. C.; Rodriguez, M. A. *Inorg. Chem.* **2000**, *39*, 5133.

(32) (a) Reich, H. J. *Chem. Rev.* **2013**, *113*, 7130. (b) Reich, H. J. *J. Org. Chem.* **2012**, *77*, 5471.

(33) Review of in situ IR spectroscopy: Rein, A. J.; Donahue, S. M.; Pavlosky, M. A. *Curr. Opin. Drug Discovery Dev.* **2000**, *3*, 734.

(34) One must be cautious in evaluating the quality of the fits to first-order formation of product $[f(x) = (a - 1)e^{-bx}]$ and second-order formation of product $(f(x) = a - a/(1 + bx))$.

(35) HMPA has been estimated to bind 300 times more strongly than THF in one case. Reich, H. J.; Kulicke, K. J. *J. Am. Chem. Soc.* **1996**, *118*, 273.

(36) We define the idealized rate law as that obtained by rounding the observed reaction orders to the nearest rational order.

(37) The rate law provides the stoichiometry of the transition structure relative to that of the reactants: (a) Edwards, J. O.; Greene, E. F.; Ross, J. *J. Chem. Educ.* **1968**, *45*, 381. (b) Collum, D. B.; McNeil, A. J.; Ramírez, A. *Angew. Chem., Int. Ed.* **2007**, *46*, 3002. (c) Meek, S. J.; Pitman, C. L.; Miller, A. J. M. *J. Chem. Educ.* **2016**, *93*, 275.

(38) Smith, B. T.; Wendt, J. A.; Aubé, J. *Org. Lett.* **2002**, *4*, 2577.

(39) Caubère, P. *Chem. Rev.* **1993**, *93*, 2317. Choppin, S.; Gros, P.; Fort, Y. *Org. Lett.* **2000**, *2*, 803.

(40) Kofron, W. G.; Baclawski, L. M. *J. Org. Chem.* **1976**, *41*, 1879.

DOI: 10.1021/jacs.7b13776
J. Am. Chem. Soc. XXXX, XXX, XXX−XXX